GEOPHYSICAL RESEARCH LETTERS, VOL. 40, 5456–5460, doi:10.1002/2013GL057797, 2013

Tasman Leakage of intermediate waters as inferred from Argo floats

Miquel Rosell-Fieschi,[1] Stephen R. Rintoul,[2,3,4,5] Jeröme Gourrion,[1] and Josep L. Pelegrí[1]

Received 26 August 2013; revised 4 October 2013; accepted 6 October 2013; published 23 October 2013.

[1] We use Argo float trajectories to infer ocean current velocity at the sea surface and 1000 dbar near Australia. The East Australian Current flows southward along the east coast of Australia at both surface and intermediate levels, but only the intermediate waters leak round the southern tip of Tasmania and cross the Great Australian Bight. We calculate the transport of Antarctic Intermediate Water (AAIW) between the southern Australian coast and the Antarctic Circumpolar Current (ACC) as the velocity at 1000 dbar times the layer thickness. Between March 2006 and December 2012, the Eulerian AAIW transport through 147°E ranges between 0 and 12.0 sverdrup (Sv). The mean Tasman Leakage of intermediate waters from the Pacific Ocean into the Indian Ocean, obtained using all Argo data until March 2013, is 3.8 ± 1.3 Sv. The mean intermediate water transport into the Indian Ocean through 115°E increases to 5.2 ± 1.8 Sv due to contributions from the westward recirculation of ACC waters. **Citation:** Rosell-Fieschi, M., S. R. Rintoul, J. Gourrion, and J. L. Pelegrí (2013), Tasman Leakage of intermediate waters as inferred from Argo floats, *Geophys. Res. Lett.*, *40*, 5456–5460, doi:10.1002/2013GL057797.

1. Introduction

[2] The global overturning circulation largely determines the capacity of the ocean to store and transport heat and carbon and thereby influence climate. Sinking of dense water in the North Atlantic and the Southern Ocean is balanced by a return flow of lighter water in the upper ocean. The existence of such a global-scale overturning circulation depends on the exchange of water masses between basins, both in the deep and upper levels of the ocean. For the upper limb, most attention has been placed on two primary pathways: the cold route through the Drake Passage [*Rintoul*, 1991] and the warm route following the Indonesian Throughflow and the Agulhas Current [*Gordon*, 1986]. A third route, the Tasman Leakage (TL), has been identified more recently [*Speich et al.*, 2001, 2002, 2007]. Repetitions of section SR3, a World Ocean Circulation Experiment (WOCE) hydrographic section between Tasmania and Antarctica, have confirmed a westward subsurface flow south of Tasmania [*Rintoul and Bullister*, 1999; *Rintoul and Sokolov*, 2001] but say nothing about its pathway to the Indian Ocean. Model studies and observations suggest that the TL provides a Pacific-to-Indian supply, a key link in a "supergyre" connecting the subtropical gyres of all Southern Hemisphere basins [*Rintoul and Sokolov*, 2001; *Sloyan and Rintoul*, 2001; *Speich et al.*, 2002; *Ridgway*, 2007; *Ridgway and Dunn*, 2007].

[3] The westward flowing South Equatorial Current (SEC) reaches the western boundary of the Pacific Ocean and bifurcates between 15°S and 20°S into northern (North Vanuatu and North Caledonia) and southern (South Caledonia) jets (Figure S1 in the supporting information). The North Caledonia (near surface) and South Caledonia (at intermediate levels) jets turn south at the Australian coast to form the East Australian Current (EAC), the western boundary current of the South Pacific subtropical gyre [*Godfrey et al.*, 1980; *Ganachaud et al.*, 2008]. In the near-surface layers, the EAC separates from the coast on its southward trip, either recirculating to form a double-cell structure [*Ridgway and Dunn*, 2003] or turning offshore at the Tasman Front or near Tasmania. Surface waters of the EAC extend farther south in summer but do not breach the southern tip of Tasmania [*Ridgway and Godfrey*, 1997]. At intermediate depths, on the other hand, part of the EAC continues south along the coast and turns west, between Tasmania and the South Tasman Rise, as the TL (Figure S1 in the supporting information). The extension of the TL into the Great Australian Bight (GAB) is known as the Flinders Current [*Middleton and Cirano*, 2002]; this subsurface transport increases as it progresses west because a fraction of the water transported by the Antarctic Circumpolar Current (ACC) recirculates westward through a large anticyclonic loop located between about 139°E and 146°E [*Rintoul and Sokolov*, 2001]. Along the southern coast of Australia, an extension of the Leeuwin Current forms a weak eastward flow of surface waters extending from Western Australia to Tasmania [*Ridgway and Condie*, 2004].

[4] Previous studies of the EAC and the TL have relied on hydrographic data or model output. In this work we use Argo float data to infer the velocity at the sea surface and 1000 dbar (the parking pressure of most Argo floats) and to estimate the thickness of the Antarctic Intermediate Water (AAIW) layer. We then combine the velocity and thickness information to quantify the variability in water transport south of Tasmania and the mean transport reaching the Indian Ocean.

2. Data and Methods

[5] The Argo float trajectories have been used to generate climatological velocity fields [*Lebedev et al.*, 2007] and to infer the current velocity in different regions [*Nuñez-Riboni et al.*, 2005; *Park et al.*, 2005; *Ollitrault et al.*, 2006; *Xie*

Additional supporting information may be found in the online version of this article.

[1]Institut de Ciències del Mar, CSIC, Barcelona, Spain.
[2]CSIRO Marine and Atmospheric Research, Hobart, Tas, Australia.
[3]Centre for Australian Weather and Climate, Hobart, Tas, Australia.
[4]Antarctic Climate and Ecosystems Cooperative Research Centre, Hobart, Tas, Australia.
[5]CSIRO Wealth from Oceans National Research Flagship, Hobart, Tas, Australia.

Corresponding author: J. L. Pelegrí, Institut de Ciències del Mar, CSIC, Barcelona ES-08003, Spain. (pelegri@icm.csic.es)

0094-8276/13/10.1002/2013GL057797

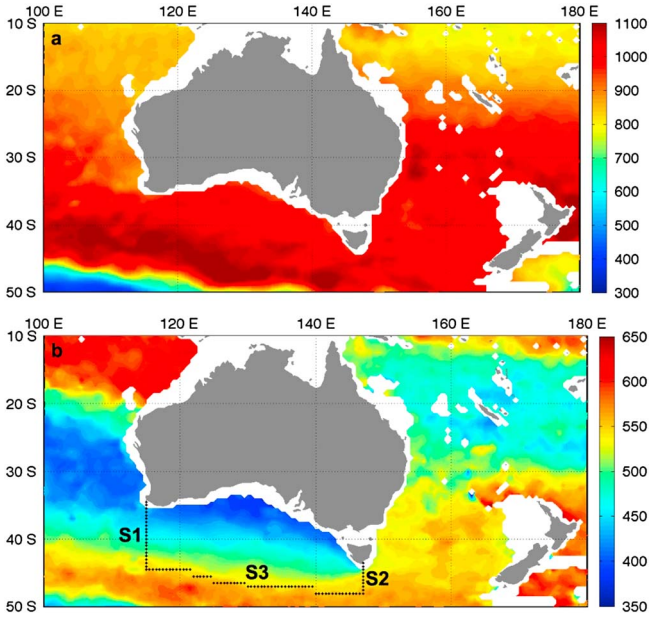

Figure 1. (a) Central level and (b) thickness of the AAIW layer (in meters), defined as having neutral densities between 27.125 and 27.6 kg m^{-3}. Figure 1b also shows the sections used to estimate the error in the transport associated to the TL.

and Zhu, 2008]. Here we use the Argo float data to produce our own velocity estimates, following the same methodology as in *Lebedev et al*. [2007]. The first and last positions of a float cycle are used to calculate the sea surface and parking depth velocities. The individual velocity estimates are spatially and temporally averaged to construct the velocity maps, with the spatial and temporal resolution depending on the amount of available data. The alternation between surface and deep drifts means that the Argo floats do not follow water parcels, so the velocity vectors inferred from the float displacements shall be understood as an Eulerian velocity measure (see the Appendix in the supporting information).

[6] While the error in surface velocity depends only on the positioning accuracy, the subsurface velocity estimates are influenced by the horizontal displacements experienced by the float during its vertical migration. *Lebedev et al*. [2007] did a detailed analysis of velocity errors at a parking pressure of 1000 dbar and concluded that the most probable relative error is 3% of the inferred value; they also concluded that 54.0% (97.6%) of the deep velocity data have relative errors less than 10% (100%) of the calculated velocity value.

[7] Here we use all delayed-mode Argo data up to March 2013, with a quality control label of "good," downloaded from the Coriolis Operational Oceanography center (www.coriolis.eu.org). We use Chauvenet's criterion [*Taylor*, 1997] to identify, and reject, spurious velocity vectors as those with either zonal or latitudinal components exceeding five standard deviations. This gives a total of 69,115 velocity vectors for the surface and 58,757 velocity vectors at 1000 dbar. The annual mean velocity is interpolated on a 1/2° × 1/2° grid, calculated from all data contained in a 100 km radius; similarly, the seasonal values are interpolated on a 1° × 1° grid, using a 150 km search radius. This generates considerable overlap between adjacent cells but increases significantly the number of velocity vectors available in each cell.

[8] The AAIW layer is defined to lie between neutral densities of 27.125 and 27.6 kg m^{-3} [*Speich et al*., 2002]. The depths of the neutral surfaces, calculated from the salinity and temperature profiles of those same Argo cycles used to compute the velocity fields, are projected on a grid following the same procedure as for the annual mean velocities. The results show that the central depth point of the AAIW layer is reasonably constant and close to 1000 dbar for the whole study area (Figure 1a), confirming that floats parked near this depth level indeed track this water mass.

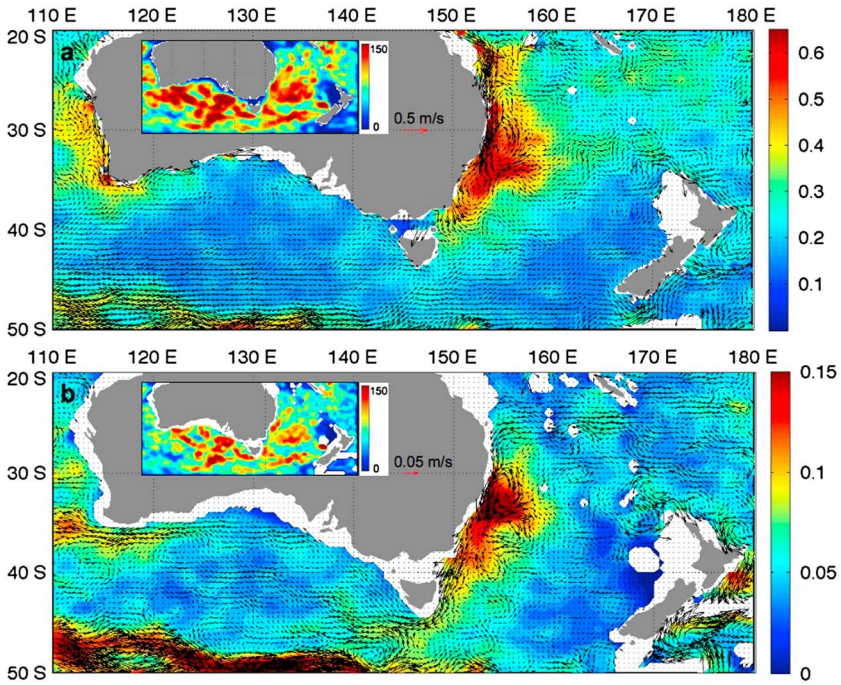

Figure 2. Mean current speed (color-coded, m s^{-1}) and current velocity vectors near Australia, both at (a) the sea surface and (b) 1000 dbar. The inset illustrates the available number of data point for each 0.5° × 0.5° cell element.

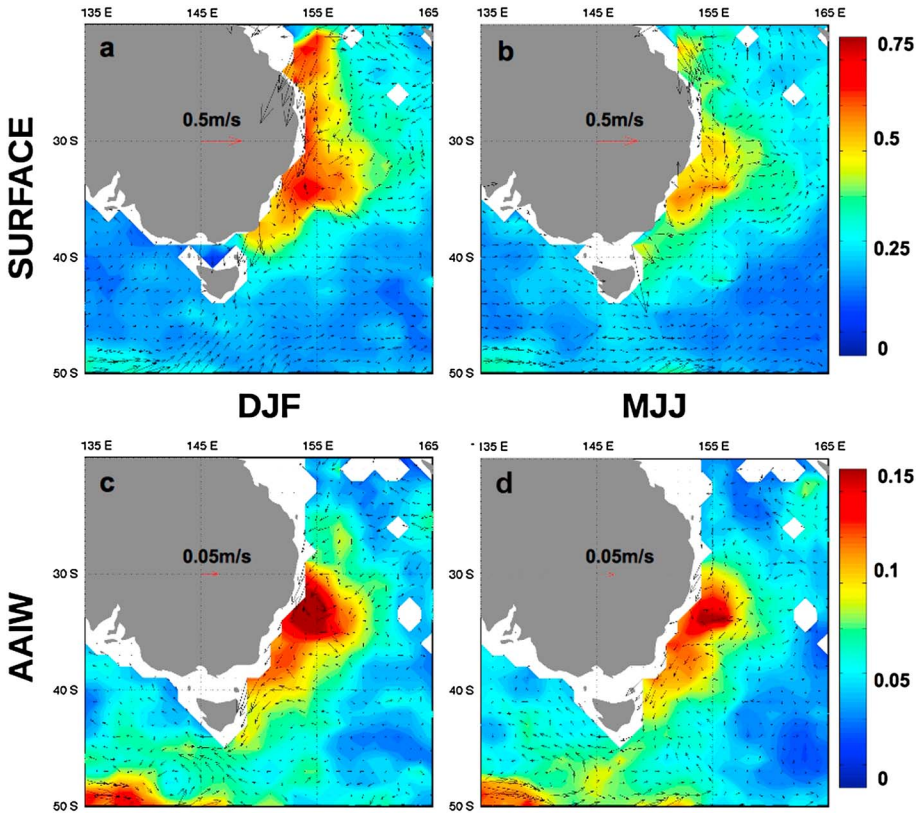

Figure 3. (a, b) Surface and (c, d) 1000 dbar monthly current speed (color-coded, m s^{-1}) and current velocity vectors for the region with the EAC and the TL; the monthly currents are calculated as 3 month averages centered on January for Figures 3a and 3c and on July for Figures 3b and 3d.

[9] The Eulerian transport is estimated by multiplying the thickness of the AAIW layer (Figure 1b) by the velocity at 1000 dbar. The numerical results of *Cirano and Middleton* [2004] endorse the assumption of a nearly constant velocity throughout the AAIW layer. In the Appendix in the supporting information, we use the divergence of the inferred velocity field to estimate a potential error of 35% in our transport estimates. We also show that this error bar is large enough to take into account possible uncertainties associated with the vertical shear of horizontal velocity within the AAIW layer and the limited sampling of relatively narrow boundary currents.

3. Results

3.1. Annual Mean

[10] The annual mean sea surface velocity map (Figure 2a) shows a double anticyclone associated with recirculations of the EAC, with a weak separation from the coast at about 32°S and a much stronger one at about 34°S, associated to the Tasman Front [*Ridgway and Dunn*, 2003]. The ultimate offshore diversion of the surface flow, however, takes place at about 40°S, so that no flow goes round the southern tip of Tasmania. The annual mean AAIW velocity map (Figure 2b) also exhibits some partial retroflection at about 34°S, but a major portion continues south and then turns west, between the Tasmania coast and the South Tasman Rise, as the TL [*Rintoul and Sokolov*, 2001; *Ridgway and Dunn*, 2007].

[11] South of Australia, the surface waters have a weak eastward flow, while the AAIW stratum predominantly moves west. The AAIW contains two different water types: a cooler and fresher variety coming from the ACC and a warmer and saltier variety supplied by the EAC. An analysis of temperature-salinity diagrams from the east and south coasts of Australia confirms the continuity of the EAC variety all the way from east to west Australia (Figure S2 in the supporting information). It also confirms that part of the AAIW carried east by the ACC recirculates to the west at lower latitudes, as observed south of Tasmania by *Rintoul and Sokolov* [2001], thereby enhancing the westward AAIW flow in the northern GAB (Figure S3).

3.2. Seasonal Variation in the EAC and the TL

[12] The surface EAC has seasonal variations greater than most midlatitude western boundary currents [*Ridgway and Godfrey*, 1997], strengthening and extending farther south during the austral summer and weakening in winter (Figures 3a, 3b, and S4). The greatest variability is associated with the northward offshore countercurrent, to the extent that the annual mean flow may be largely accomplished by eddies [*Ridgway and Godfrey*, 1997; *Ridgway and Dunn*, 2003]. One cause for such variability may be the seasonal cycle of the impinging SEC, which feeds the EAC [*Sokolov and Rintoul*, 2000]. Another reason may be the variable extension of the Leeuwin Current across the GAB [*Ridgway and Godfrey*, 1997]: During the austral winter and spring, this current rounds the southern tip of Tasmania and flows along its eastern coast as the northward extension of the Zeehan Current, possibly blocking the southward progression of the EAC.

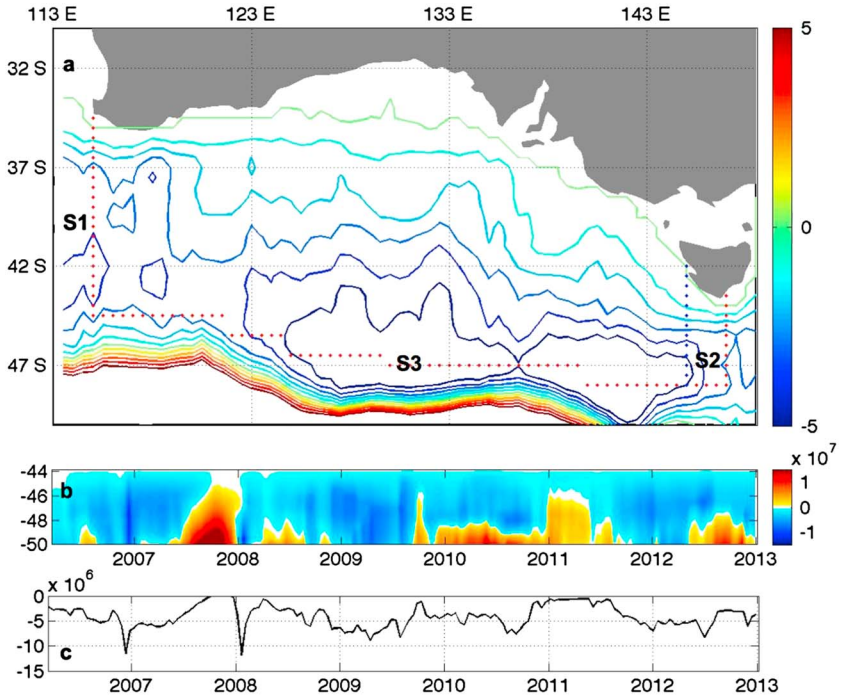

Figure 4. (a) Annual mean AAIW streamlines south of Australia; zero is taken at the coast, and increasing negative values represent westward transport (Sv). Sections S1 (115°E) and S2 (147°E) are shown as red dotted lines; the blue dotted lines coincide with 145°E, where *Speich et al*. [2007] did their transport calculations. (b) AAIW transport across 147°E (Sv), integrated south from Tasmania, as a function of time and latitude; values are obtained using a 5 month running filter with a search radius of 150 km and gridding on 1° cells. (c) Time series of the maximum westward transports (negative values, Sv) in Figure 4b. Tick marks in Figures 4b and 4c indicate the beginning of the calendar year.

[13] In contrast to the strong seasonality of the surface flow, the EAC and its westward TL extension are remarkably steady at the AAIW level during all seasons (Figures 3c, 3d, and S4). Nevertheless, the subsurface EAC also experiences seasonal changes, as its northern portion strengthens during austral spring and autumn and the southern portion gains intensity during austral winter and summer. This may be related to the alternation in the intensity of those jets (North Vanuatu, North Caledonia, and South Caledonia) feeding the EAC [*Ganachaud et al*., 2008].

4. Intermediate Water Mass Transport by the TL

[14] There have been several attempts at estimating the magnitude of the TL. The first geostrophic calculations, from repeated SR3 WOCE sections, gave a transport of 8 ± 13 sverdrup (Sv) for the whole water column [*Rintoul and Sokolov*, 2001]. Early results by *Speich et al*. [2002] quantified the TL as the result of 13 ± 3 Sv of Subantarctic Mode Water (SAMW) and 26 ± 4 Sv of AAIW; however, only a fraction of this transport, 3.7 ± 2.5 Sv of SAMW and 10 ± 3 Sv of AAIW, reached the Indian Ocean. Later model computations by *Speich et al*. [2007] found a Lagrangian mean transport of 3.2 Sv of intermediate waters all the way to the North Atlantic. *Davis* [2005], from a limited number of float trajectories near 1000 dbar and assuming an AAIW thickness of 500 m, estimated a leakage of 7.5 Sv from the Pacific Ocean to the Indian Ocean.

[15] Here we estimate both the TL and ACC contributions to the intermediate water transport into the Indian Ocean. We limit our calculations to the region north of the ACC, as the AAIW layer shoals rapidly to the south (Figure 1a). The accumulated annual mean zonal transport is calculated every 0.5° between sections S2 (147°E) and S1 (115°E), i.e., along the whole GAB, integrating south from the Australian coast (Figure 4a). These accumulated transports, equivalent to streamlines for the AAIW layer, reveal the path of the TL from the Pacific Ocean to the Indian Ocean and the appearance of contributions due to the recirculation of ACC. We find an Eulerian mean transport of 3.8 ± 1.3 Sv across 147°E. A significant ACC input (1.2 Sv) occurs between 145°E and 147°E, provided by the eastern limb of a large anticyclonic gyre which extends from about 123°E to 146°E. The transport entering the Indian Ocean is estimated as 5.2 ± 1.8 Sv, being the result of three contributions: the TL through 147°E (3.8 Sv), water escaping westward from the anticyclone between 123°E and 146°E (0.4 Sv), and water recirculating in the southwestern end of our domain (1.0 Sv).

[16] The number of Argo floats south of Tasmania allows estimating changes in water transport through section 147°E, at temporal scales influenced by eddies. We calculate the accumulated transports south of Tasmania, every 15 days, between March 2006 and December 2013; for this calculation, we use a running interval of 150 days (5 months) as a characteristic time scale for eddies in this region [*Herraiz-Borreguero and Rintoul*, 2011] (Figure 4b). The negative values are a measure of the Eulerian TL transport at each time, which varies between 0 and −12.0 Sv, with a mean value of −4.4 Sv and a standard deviation of 2.8 Sv (Figure 4c); this variability reflects the high eddy activity along 147°E, as suggested by *van Sebille et al*. [2012] from numerical models. Given the thickness h, width d, and speed u of the westward AAIW

flowing waters, so that the cross-sectional transport area is $A = h\,d$, we may decompose the mean transport $\overline{A\,u} = -4.4$ Sv as contributions from the mean values and their fluctuations, $\overline{A\,u} = \overline{A}\,\overline{u} + \overline{A'u'}$. Computing $\overline{A}\,\overline{u} = -2.7$ Sv, we estimate the eddy contribution to be $\overline{A'u'} = -1.7$ Sv, or 39% of the total transport.

5. Conclusions

[17] Velocity data inferred from Argo float trajectories are used to characterize the currents near Australia at the sea surface and 1000 dbar levels. The inferred flow field agrees with the geostrophic circulation as estimated from a hydrographic climatology and a level of no motion [*Ridgway and Dunn*, 2003]. The circulation off eastern Australia is dominated at both levels by the EAC. However, only the intermediate waters turn around the southern tip of Tasmania and flow west into the GAB. We find that the subsurface extension of the EAC supplies the TL and, ultimately, the Pacific-to-Indian link of the Southern Hemisphere supergyre.

[18] These observations are the first direct measurements of the intermediate-depth circulation near Australia with adequate spatial resolution to resolve boundary currents and their recirculations and sufficient temporal resolution to account for the seasonal cycle. The westward Eulerian transport south of Tasmania displays substantial variability, likely due to the presence of eddy activity, between times of no leakage to maximum values of 14.5 Sv. We estimate the mean leakage of AAIW into the Indian Ocean to be 3.8 ± 1.3 Sv. Between 147°E and 145°E, the mean water transport increases to 5.0 ± 1.8 Sv because of the contribution from an anticyclonic gyre north of the ACC, and at 115°E, the mean net westward transport is 5.2 ± 1.8 Sv.

[19] **Acknowledgments.** Funding for this work comes from the Spanish Ministerio de Ciencia e Innovación through project "Tipping Corners in the Meridional Overturning Circulation" (TIC-MOC, reference CTM2011-28867). Miquel Rosell-Fieschi would also like to acknowledge the Ministerio de Ciencia e Innovación for funding through a FPU grant. This work was supported in part by the Australian Government's Cooperative Research Centres Program, through the Antarctic Climate and Ecosystems Cooperative Research Centre (ACE CRC), and by the Department of Climate Change and Energy Efficiency, through the Australian Climate Change Science Program.

[20] The Editor thanks Sabrina Speich and an anonymous reviewer for their assistance in evaluating this paper.

References

Cirano, M., and J. F. Middleton (2004), Aspects of the mean wintertime circulation along Australia's southern shelves, *J. Phys. Oceanogr.*, *34*, 668–684.

Davis, R. E. (2005), Intermediate-depth circulation of the Indian and South Pacific Oceans measured by autonomous floats, *J. Phys. Oceanogr.*, *35*, 683–707.

Ganachaud, A., L. Gourdeau, and W. Kessler (2008), Bifurcation of the subtropical South Equatorial Current against New Caledonia in December 2004 from a hydrographic inverse box model, *J. Phys. Oceanogr.*, *38*, 2072–2084.

Godfrey, J. S., G. R. Cresswell, T. J. Golding, and A. F. Pearce (1980), The separation of the East Australian Current, *J. Phys. Oceanogr.*, *10*, 430–440.

Gordon, A. L. (1986), Interocean exchange of thermocline water, *J. Geophys. Res.*, *91*, 5037–5046.

Herraiz-Borreguero, L., and S. R. Rintoul (2011), Regional circulation and its impact on upper ocean variability south of Tasmania, *Deep Sea Res., Part II*, *58*, 2071–2081.

Lebedev, K. V., H. Yoshinari, N. Maximenko, and P. W. Hacker (2007), YoMaHa'07: Velocity data assessed from trajectories of Argo floats, IPRC Tech. Note 4(2), 20 pp.

Middleton, J. F., and M. Cirano (2002), A northern boundary current along Australia's southern shelves: The Flinders Current, *J. Geophys. Res.*, *107*(C9), 3129, doi:10.1029/2000JC000701.

Nuñez-Riboni, I., O. Boebel, M. Ollitrault, Y. You, P. L. Richardson, and R. Davis (2005), Lagrangian circulation of Antarctic Intermediate Water in the subtropical South Atlantic, *Deep Sea Res., Part II*, *52*, 545–564.

Ollitrault, M., M. Lankhorst, D. Fratantoni, P. Richardson, and W. Zenk (2006), Zonal intermediate currents in the equatorial Atlantic Ocean, *Geophys. Res. Lett.*, *33*, L05605, doi:10.1029/2005GL025368.

Park, J. J., K. Kim, B. A. King, and S. C. Riser (2005), An advanced method to estimate deep currents from profiling floats, *J. Atmos. Oceanic Technol.*, *22*, 1294–1304.

Ridgway, K. R. (2007), Seasonal circulation around Tasmania—An interface between eastern and western boundary dynamics, *J. Geophys. Res.*, *112*, C10016, doi:10.1029/2006JC003898.

Ridgway, K. R., and S. A. Condie (2004), The 5500-km-long boundary flow off western and southern Australia, *J. Geophys. Res.*, *109*, C04017, doi:10.1029/2003JC001921.

Ridgway, K. R., and J. R. Dunn (2003), Mesoscale structure of the mean East Australian Current system and its relationship with topography, *Progr. Oceanogr.*, *56*, 189–222.

Ridgway, K. R., and J. R. Dunn (2007), Observational evidence for a southern hemisphere oceanic supergyre, *Geophys. Res. Lett.*, *34*, L13612, doi:10.1029/2007GL030392.

Ridgway, K. R., and J. S. Godfrey (1997), Seasonal cycle of the East Australian Current, *J. Geophys. Res.*, *102*, 22,921–22,936.

Rintoul, S. R. (1991), South Atlantic interbasin exchange, *J. Geophys. Res.*, *96*, 2675–2692.

Rintoul, S., and J. Bullister (1999), A late winter hydrographic section from Tasmania to Antarctica, *Deep Sea Res., Part I*, *46*, 1417–1454.

Rintoul, S., and S. Sokolov (2001), Baroclinic transport variability of the Antarctic Circumpolar Current south of Australia (WOCE repeat section SR3), *J. Geophys. Res.*, *106*, 2815–2832.

Sloyan, B., and S. Rintoul (2001), The Southern Ocean limb of the global deep overturning circulation, *J. Phys. Oceanogr.*, *31*, 143–173.

Sokolov, S., and S. Rintoul (2000), Circulation and water masses of the southwest Pacific: WOCE Section P11, Papua New Guinea to Tasmania, *J. Mar. Res.*, *58*, 223–268.

Speich, S., B. Blanke, and G. Madec (2001), Warm and cold water routes of an OGCM thermohaline conveyor belt, *Geophys. Res. Lett.*, *28*, 311–314.

Speich, S., B. Blanke, P. de Vries, S. Drijfhouté, K. Döös, A. Ganachaud, and R. Marsh (2002), Tasman leakage: A new route in the global ocean conveyor belt, *Geophys. Res. Lett.*, *29*(10), 1416, doi:10.1029/2001GL014586.

Speich, S., B. Blanke, and W. Cai (2007), Atlantic meridional overturning circulation and the Southern Hemisphere supergyre, *Geophys. Res. Lett.*, *34*, L23614, doi:10.1029/2007GL031583.

Taylor, J. (1997), *An Introduction to Error Analysis: The Study of Uncertainties in Physical Measurements*, 2nd ed., pp. 166–168, Univ. Sci. Books, Sausalito, Calif.

Van Sebille, E., M. H. England, J. D. Zika, and B. N. Sloyan (2012), Tasman leakage in a fine-resolution ocean model, *Geophys. Res. Lett.*, *39*, L06601, doi:10.1029/2012GL051004.

Xie, J., and J. Zhu (2008), Estimation of the surface and mid-depth currents from Argo floats in the Pacific and error analysis, *J. Mar. Syst.*, *73*, 61–75.